Silicon-Based Chemical Motors: An Efficient Pump for Triggering and Guiding Fluid Motion Using Visible Light

Maria J. Esplandiu,*,†,‡ Ali Afshar Farniya,† and Adrian Bachtold§

†Institut Catala de Nanociencia i Nanotecnologia, Campus UAB, 08193 Bellaterra, Barcelona, Spain, ‡Consejo Superior de Investigaciones Científicas, ICN2 Building, Campus UAB, 08193 Bellaterra, Barcelona, Spain, and §Institut de Ciencies Fotoniques, Mediterranean Technology Park, 08860 Castelldefels, Barcelona, Spain

ABSTRACT We report a simple yet highly efficient chemical motor that can be controlled with visible light. The motor made from a noble metal and doped silicon acts as a pump, which is driven through a light-activated catalytic reaction process. We show that the actuation is based on electro-osmosis with the electric field generated by chemical reactions at the metal and silicon surfaces, whereas the contribution of diffusio-osmosis to the actuation is negligible. Surprisingly, the pump can be operated using water as fuel. This is possible because of the large ζ-potential of silicon, which makes the electro-osmotic fluid motion sizable even though the electric field generated by the reaction is weak. The electro-hydrodynamic process is greatly amplified with the addition of reactive species, such as hydrogen peroxide, which generates higher electric fields. Another remarkable finding is the tunability of silicon-based pumps. That is, it is possible to control the speed of the fluid with light. We take advantage of this property to manipulate the spatial distribution of colloidal microparticles in the liquid and to pattern colloidal microparticle structures at specific locations on a wafer surface. Silicon-based pumps hold great promise for controlled mass transport in fluids.

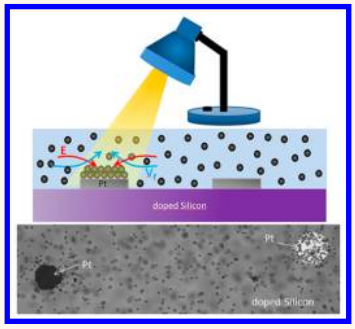

KEYWORDS: catalytic motors · electro-hydrodynamic forces · chemomechanical actuation · photoactivation

Development of artificial and autonomous nanomachines is a topic of great interest with significant impact in numerous engineering applications, such as nano- and micro-electromechanical systems, fluid pumping, chemical sensing, particle assembly, drug delivery, and nanophotonics.[1−12] The use of light to control motion is very attractive given its fast switchable capabilities. Mechanically interlocked molecular architectures based on rotaxanes and catenanes represent pioneer systems on which UV-light-driven motion has been probed.[13−17] These systems are synthesized with precisely tailored structures and functions to act as rotors, gears, switches, and shuttles. There has been considerable effort to demonstrate that these molecular motors can perform large-scale and useful mechanical work based on the cumulative nanoscale movement of molecular machine assemblies. This includes the macroscale transport of liquids onto surfaces modified with UV-light-driven molecular switches,[18] shape changes of elastomers embedded with molecular switches,[19−21] and drug delivery particles modified with molecular motors acting as nanovalves.[17]

The emergence of catalytic motors has opened a broad range of novel devices which can be actuated chemically and photochemically with UV light. Photochemical-driven motors have been developed either in a pump configuration or as self-propelled particles. Motors made of UV photoactive materials, such as Ag, AgCl, Ag_3PO_4, and TiO_2, can be actuated either in H_2O_2 solutions or in water.[22−31] The chemical species released during the photoreaction at the motor surface generate ion concentration gradients which power the motion by self-diffusiophoresis. The use of UV light also triggers attractive and repulsive interactions among active particles, inducing collective behaviors. This phenomenon has been rooted to the overlap of the ion concentration gradients of interacting active motors, which promote their communication and cooperation in a similar way as nature does in the processes of chemotaxis and phototaxis. Photochemically induced motion of particles has also been generated through other mechanisms such as bubble recoil.

* Address correspondence to mariajose.esplandiu@cin2.es.

Received for review August 4, 2015 and accepted September 8, 2015.

Published online September 08, 2015
10.1021/acsnano.5b04830

For instance, liquid metal droplets coated with WO_3 nanoparticles exhibit motion when placed in H_2O_2 solution and under UV illumination.[32] The photoreaction generates oxygen bubbles that propel the metal droplet.

Many motors powered by UV light degrade with time, which limits their lifetime.[23,24,27] For instance, the actuation mechanism of Ag-based motors is based on their own photocorrosion. Moreover, there are other systems that can also suffer surface degradation by the combined effect of the high-energy wavelengths and the chemical fuel. An interesting alternative to UV propulsion has been reported very recently, in which hematite swimmers[33,34] were activated using blue light. In this context, it would be promising to find a robust strategy in order to activate the actuation of catalytic motors with visible light. In addition, there has been a report in which visible light was used not to propel catalytic motion but instead to stop it.[35]

We have developed a simple yet powerful and robust silicon-based photocatalytic motor that can be controlled with visible light. Moreover, this motor can by fueled simply by water. Actuation with water is possible because of the large ζ-potential of silicon, which makes the electro-osmotic fluid motion sizable even though the electric field generated by the reaction is weak. The electro-hydrodynamic process is greatly amplified if reactive fuels such as hydrogen peroxide are employed. Equally fascinating is that light can be used to control mass transport in liquid in an unprecedented manner. The photo-chemomechanical actuation can be harnessed to efficiently guide material to precise locations on a substrate.

RESULTS AND DISCUSSION

Catalytic pumps consist of 30−50 μm diameter platinum disks and with a Pt thickness of 50 nm patterned on top of doped silicon wafers. The fabrication was achieved using electron beam lithography and electron beam evaporation, followed by an oxygen plasma treatment in order to clean the surface.[36,37] The flow of the liquid driven by the pumps was characterized by monitoring the motion of particle tracers using an optical microscope. Particles with different charges were used in order to be able to quantify the electric field generated by the pumps. Amidine-modified polystyrene particles, plain polystyrene particles, and silica particles were used as positive, quasi-neutral, and negative tracers.

We first present measurements of pumps immersed just in water. The particle motion in the region in the vicinity of the pump was triggered by illuminating this region with the white light of the optical microscope. Positive particles (P^+) move toward the platinum disk. Once arrived at the disk, they stick to the surface, as observed in Figure 1a. The radial velocity increases as the particles come closer to the disk. In the vicinity of the platinum−silicon border, the average velocity reaches its maximum value, $12.0 \pm 2.5\ \mu m \cdot s^{-1}$. Quasi-neutral ($P^0$) particles also move toward the disk, but after having crossed the platinum−silicon border, they turn by 90° and flow upward in the direction opposite to the surface. The particles reach a maximum radial velocity of $8.5 \pm 1.3\ \mu m \cdot s^{-1}$ close to the border (Figure 1b). Negative particles (P^-) are repelled from the Pt disk. Movies of the motion of the different charged particles are incorporated in the Supporting Information. Importantly, no motion of particles is observed if an insulating layer of aluminum oxide (20 nm thickness) or silicon oxide (450 nm thickness) is placed between the metal and the doped silicon surface. This finding proves that transfer of electrons between the semiconductor and the metal is mandatory to make this pump operative. This experimental finding also suggests that the actuation of these metal−semiconductor pumps is based on electro-osmosis, as in previous studies on pumps based on metal disks patterned onto metal surfaces.[36,38] In such an electro-osmosis actuation, the electric field is generated by the gradient of charged species in the liquid, which results from the different chemical reactions occurring at the silicon−water interface and the platinum−water interface. This is a remarkable finding since it proves that water could have chemical fuel capabilities for catalytic pumps.

In order to get more insight into the electro-osmosis actuation, we used confocal fluorescence microscopy with a proton indicator dye. Protons are the typical species involved in electrochemical reactions. The measurements were performed using pyranine as the fluorescent probe and under ratiometric conditions (see Supporting Information).[36] Figure 1c shows the existence of a proton gradient near the disk. High proton concentration is produced on the silicon side, whereas the proton concentration is decreased on the metal side. Although the exact nature of the photocatalytic reactions is not known, the production of protons could be related to some oxidation reactions mediated by water at the silicon interface, whereas the proton decrease on the metal side could possibly be related to the reduction of oxygen, a process that consumes protons. By contrast, no proton gradient is generated when an insulating layer is placed between the metal and the semiconductor, as depicted in Figure 1d. According to these fluorescence measurements and the behavior of the differently charged particles, the electric field points from the silicon (anode) to the metal (cathode) and the fluid flows in the same direction (Figure 1c). We confirmed the existence of such electric field by adding salt. A decrease of the speed of the particles is observed, which indicates the screening of the electric field by the salt (see Figure S2 in the Supporting Information).

The electric field and the fluid flow can be estimated from the radial velocities of the positive and

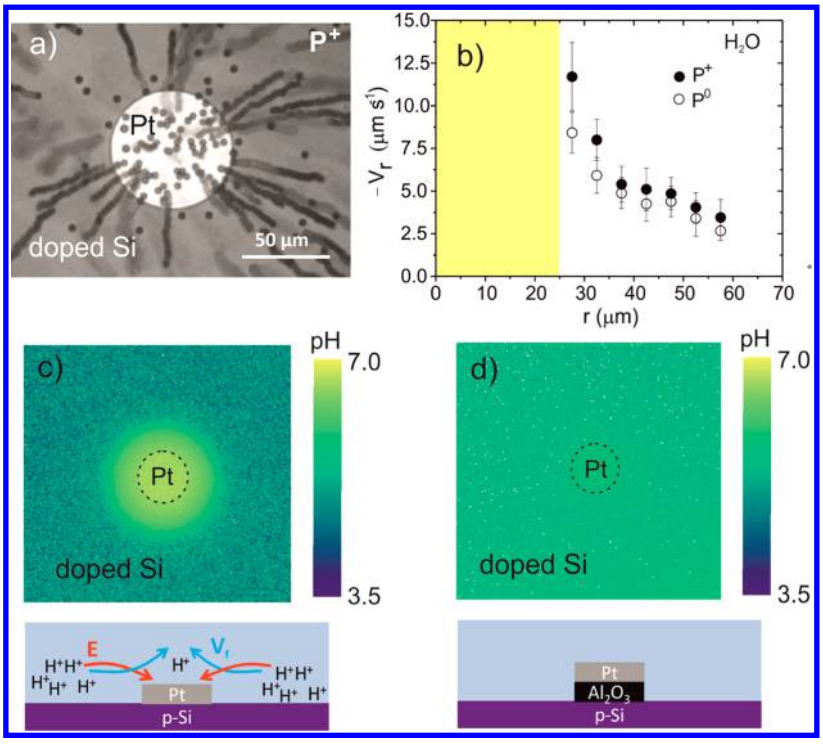

Figure 1. (a) Tracking of positive particles using a p-Si/Pt pump in pure water. The P^+ particles move toward the platinum disk center and settle on it. The figure is the superposition of 80 images recorded with the optical microscope every 0.2 s. (b) Average radial velocity (V_r) of P^+ and P^0 particles as a function of the radial component in water. The yellow area represents the area of the platinum disk. The origin point is the center of the Pt disk. The diameter of the disk is 50 μm. The curve for P^+ particles represents the averaged data of four devices and 20 particles. The curve for P^0 particles represents the averaged data of three devices and 17 particles. (c) Image of the pH gradient obtained from fluorescence ratiometric measurements using pyranine as the pH indicator together with a schematic showing the pump with the proton gradient and the direction of electric field and fluid flow. (d) Map of the pH distribution when 20 nm of an insulating layer (Al_2O_3) is placed between the semiconductor and the metal, as illustrated in the scheme below the figure.

quasi-neutral particles ($V_r(r)$) using eq 1, which considers the electrophoretic contribution of the particle and the fluid flow (V_f).

$$V_r(r) = \frac{\varepsilon\zeta_p}{\eta} E_r(r) + V_f(r) \quad (1)$$

where $E_r(r)$ is the radial electric field strength, ζ_p is the ζ-potential of the particles, and ε and η are the fluid dielectric constant and viscosity, respectively.[36,37] The maximum values of V_f and E_r obtained at the Pt border are 8.9 $\mu m \cdot s^{-1}$ and 80 $V \cdot m^{-1}$, respectively. This electric field is much smaller than the one we measured on metal−metal pumps,[36,37] typically on the order of 300 $V \cdot m^{-1}$. In the semiconducting metal pumps studied here, the particle motion is made possible because of the comparatively large liquid flow term in eq 1. This is rooted to the high negative ζ-potential of the silicon surface ($\zeta_{p,surface} < -40$ mV), which is involved in the fluid flow term

$$V_f(r) = -\frac{\varepsilon\zeta_{surface}}{\eta} E_r(r) \quad (2)$$

Adding hydrogen peroxide to the water greatly amplifies the actuation of silicon-based pumps. Figure 2 shows the characterization of the device in the presence of 1 wt % hydrogen peroxide with positive, quasi-neutral, and negative particles. The charged particles follow the same trends as those obtained previously in the presence of water. Positive particles move toward the Pt disk and stick on it (Figure 2a); quasi-neutral particles move toward the Pt disk and then upward following the fluid flow (Figure 2b), and negative particles are repelled from the Pt disk (Figure 2c), forming a large repulsive region. Movies of the motion of the different particles in H_2O_2 have been added in the Supporting Information. Positively charged particles acquire high velocities even at far distances from the platinum disk, as depicted in Figure 2d. A maximum average velocity of 65.4 ± 8.5 $\mu m \cdot s^{-1}$ is achieved near the platinum−silicon boundary. Maximum values of 43 $\mu m \cdot s^{-1}$ and 680 $V \cdot m^{-1}$ were estimated for V_f and E_r, respectively, at the Pt edge using eq 1, which highlights the amplification effect of H_2O_2 in the photochemical actuation. Figure 3a shows the decrease of the positive particle velocity when adding different concentrations of KCl, indicating that salt screens the electric field.

We could not observe the motion of particles when an insulating layer was placed between the semiconductor and the metal. This indicates that the contribution of diffusio-osmosis to the actuation is negligible. Indeed, the diffusio-osmosis process could lead to the

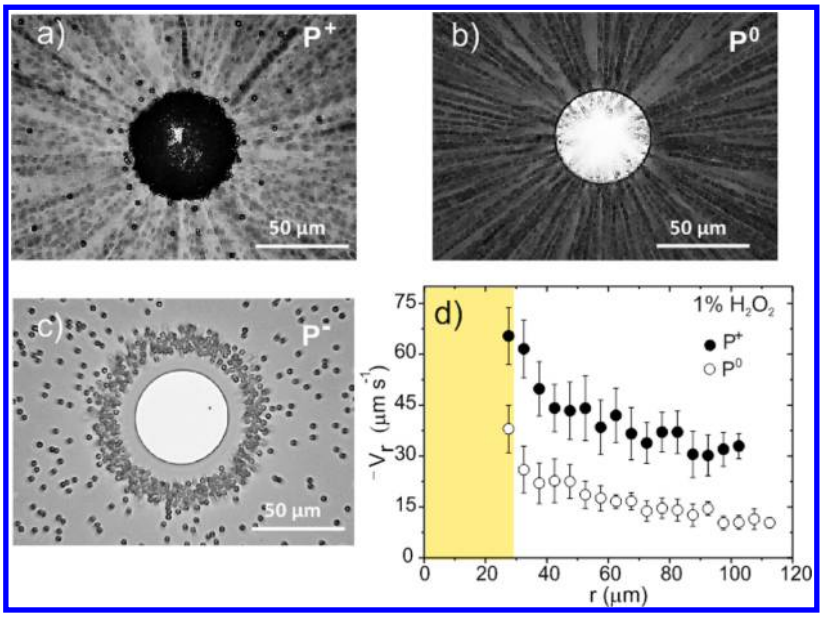

Figure 2. Motion of (a) positive, (b) quasi-neutral, and (c) negative particles using a p-doped Si/Pt pump in 1% H_2O_2. Positive particles stick on the Pt disk. The black color of the disk is due to the accumulation of particles. The quasi-neutral P^0 particles move toward the platinum disk. After having crossed the Si−Pt border, they are pushed upward. The figures are the superposition of 45 images recorded with the optical microscope every 0.2 s. (d) Average radial velocity (V_r) of P^+ and P^0 particles as a function of the radial component in H_2O_2. The yellow area represents the area of the platinum disk. The diameter of the disk is 50 μm. The velocity plot for P^+ particles is based on the averaged data of eight devices and 28 particles. The plot for P^0 tracers has been obtained by processing three devices and 19 particles.

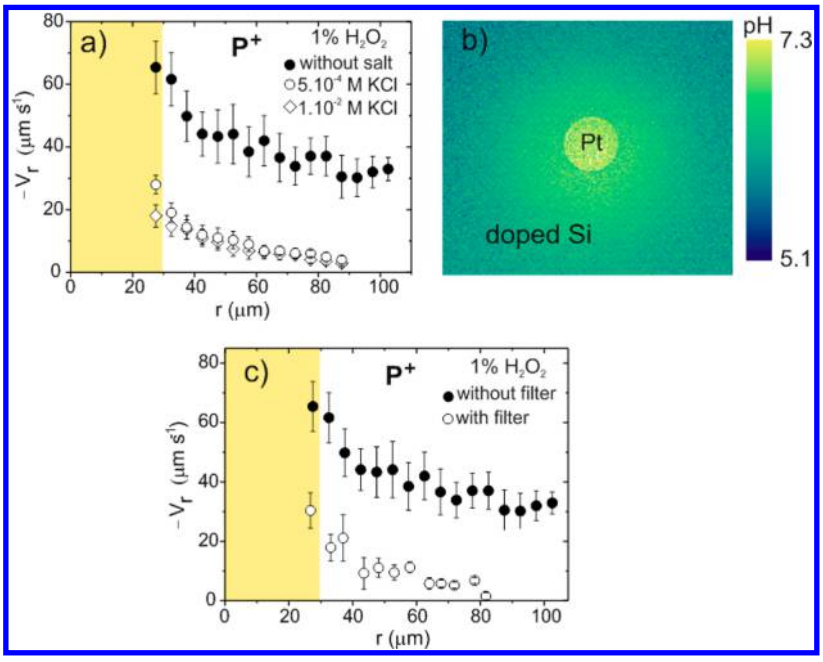

Figure 3. (a) Effect of potassium chloride concentration on the average radial velocity of positive particles in 1 wt % hydrogen peroxide. (b) Map of the proton gradient in the presence of H_2O_2. (c) Effect of light intensity on the average radial velocity of positive particles in 1 wt % hydrogen peroxide solution.

motion of particles even in the presence of an electrical insulator placed between the metal and the silicon due to the non-electrochemical decomposition of hydrogen peroxide on Pt ($2H_2O_2 \rightarrow 2H_2O + O_2$);[39] the asymmetrical distribution of the concentration of neutral chemical species produced by such reactions could actuate the fluid flow.[40] Since this is not the case, we can consider that the actuation is solely based on electro-osmosis. This result is important regarding the growing debate on the nature of the propulsion of Janus particles. Neutral self-diffusiophoresis was first proposed to be the main mechanism behind the propulsion of Janus particles made of insulator and platinum structures due to the non-electrochemical

decomposition of H_2O_2.[39] However, it was later argued that the particles are propelled by an electrokinetic process.[41] This has opened an intense discussion on the nature of the chemomechanical actuation of insulator/metal motors in the presence of H_2O_2.[41,42]

In order to confirm that proton generation and consumption are taking place during the photoelectrochemical decomposition of hydrogen peroxide, we have also imaged the proton concentration using the pyranine fluorescent dye, as illustrated in Figure 3b. A proton gradient is observed with higher proton concentration at the silicon surface. The figure only shows a qualitative trend of the proton gradient since the photobleaching of the dye increased in the presence of hydrogen peroxide under illumination.

To characterize the effect of light on the actuation, we performed experiments at different light intensities and frequencies. Figure 3c shows the motion of positively charged particles for two different illumination intensities. A neutral density (ND) filter with the capability to reduce the intensity by 75% over the whole visible spectrum was used. The velocity of the particles drops as the light intensity is decreased. We also checked the response of p-doped Si/Pt pumps for different excitation wavelengths, 405, 488, 561, and 633 nm. The variation of the velocity of positive particles does not change much upon varying the wavelength (Figure S4 in Supporting Information). We also found that the silicon substrate has to be doped in order to activate the photoactuation with light in the visible range. Pumps made of n-doped silicon/Pt or doped silicon/Au showed performance similar to that of p-Si/Pt devices (see movie and Figure S3 in the Supporting Information).

We now discuss the microscopic nature of the observed photodriven chemomechanical mechanism. A possible scenario is that light increases the chemical reaction rate by enhancing the formation of electron/hole pairs. This is the typical phenomenon occurring in photocatalysis mediated by semiconductors.[43,44] More specifically, photons excite electrons from the valence band to the conduction band, leaving holes in the valence band. These holes can be strong oxidizing agents for the species in the fluid producing protons (Figure 4), as demonstrated in refs 43 and 44. The excited electrons decay nonradiatively and diffuse toward the metal surface through the doped silicon substrate. These electrons then participate in the reduction reaction occurring at the metal surface (Figure 4). As a result, a gradient of proton concentration is formed in the fluid, so that the associated electric field drives the motion of the fluid through electro-osmosis.[36] Such a scenario is consistent with the observed increase of the fluid velocity upon enhancing the light intensity. In addition, the light could increase the temperature at the interface, which would also enhance the reaction kinetics.

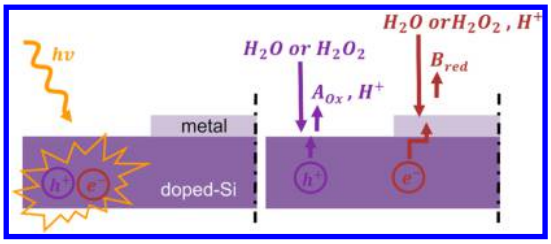

Figure 4. Schematics illustrating the possible mechanism of the photoactivated catalytic reactions of doped silicon/metal pumps. The light absorption generates electron and hole pairs. The holes oxidize species of the fluid, and the electrons are transferred to the metal, where the reduction of the fluid takes place.

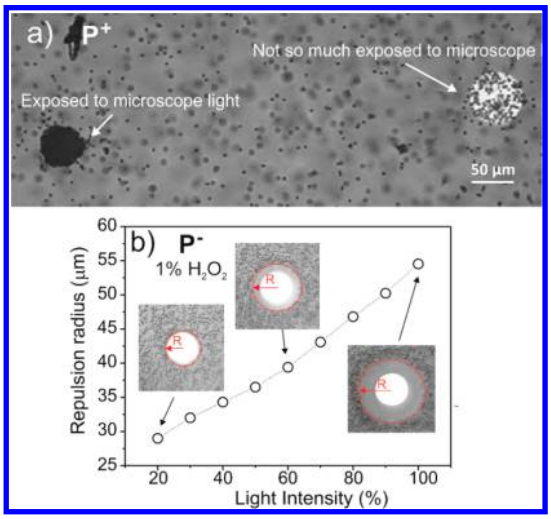

Figure 5. (a) Effect of light exposure on patterning the platinum disk with positive particles on p-Si/Pt devices in 1 wt % hydrogen peroxide. The disk on the left side was extensively exposed to the microscope light so that it was completely covered with positive particles. Only few particles settled on the right disk, which was not much exposed to the microscope light. The left disk was exposed with a light intensity that is 8.4 larger than that used to expose the right disk; the ratio in the exposure dose between the left disk and the right disk was 84. (b) Radius of the repulsion band as a function of light intensity when the pump was immersed in a solution of hydrogen peroxide with negatively charged particles.

We now show how silicon pumps can be used to manipulate the spatial distribution of particles in the liquid and to pattern particle structures at specific locations on the surface. The image in Figure 5a shows a sample with two platinum disks patterned on the substrate and immersed in a 1% H_2O_2 solution with positive particles. The platinum disk on the left side was intensively exposed to the microscope light (by zooming the field of view) and was completely covered with P^+ particles. Only a few particles settled on the other disk, which was exposed with a much lower dose. This shows that a selective control of particle patterning on specific disks can be achieved by illuminating different locations of the sample.

The light can also be employed to modify the spatial distribution of particles diffusing in the liquid upon

varying the light intensity. Figure 5b shows that negatively charged particles are repelled away from the disk, forming a so-called repulsion band without any particles. Upon varying the light intensity, the radius of the band can be changed. This motion of negatively charged particles is reversible at will. Here, the radial distance is taken from the center of the Pt disk to the particle front. The response of the band radius to changes in the light intensity is rapid, on the order of 1 s (Figure S5 in Supporting Information).

CONCLUSIONS

The combination of doped silicon and metal represents an exciting strategy for the design of chemical motors triggered by visible light. The pumps that we fabricated can be simply actuated in water. The electrohydrodynamic forces are greatly amplified when using chemically reactive fuels, such as hydrogen peroxide. The highly efficient chemomechanical actuation is the result of the highly negative ζ-potential of the doped silicon surface. Our experimental findings indicate that the process relies on the photoactivated chemical reactions at the silicon and the metal surfaces, with silicon acting as the anode and the metal as the cathode. The physical nature of the photoactivation mechanism is not fully understood, but it could share similarities with the processes of photocatalysis on semiconducting surfaces. Our findings prove that light is a promising tool to modulate and guide motion of colloid particles in a controllable and fast way. These results constitute the proof-of-concept of a novel control of matter in liquid, which can open new and promising research activities in the field of catalytic actuators and nanomotors.

MATERIALS AND METHODS

The fabricated pumps consist of 30−50 μm diameter Pt or Au disks patterned on doped silicon wafers (with a resistivity of 1−20 $\Omega\cdot$cm) using standard electron beam lithography and electron beam evaporation. An adhesion layer of chromium was deposited between the metal disk and the silicon. The devices were subjected to 1 min of plasma cleaning (360 W) to remove organic contamination. An 8 mm diameter and 0.12 mm thick gasket-like spacer (Invitrogen) was placed on top of the wafer patterned with pumps. Either water or 1% hydrogen peroxide solution containing differently charged microparticles was added to the vacant space created by the gasket. The wafer was immediately capped with a thin glass cover. We used positively charged particles made from polystyrene spheres functionalized with amidine groups (Invitrogen, ζ_{P+} = 46 mV), negatively charged particles from pristine silica (Kisker Biotech GmbH & Co., ζ_{P-} = −83 mV), and quasi-neutral particles from pristine polystyrene spheres (Kisker Biotech GmbH & Co., ζ_{P0} = −12 mV). The diameter of all the particles is 2 μm. The ζ-potential of the particles was measured with a Zetaseizer Nano-ZS (Malvern Instruments) based on electrophoretic light scattering. The ζ-potential of the doped silicon surface was estimated using doped silicon rods immersed in water. Values around −45 mV were obtained in this case. The particle motion was optically recorded with a rate of 5 frames per second and analyzed with the Diatrack software to determine the radial velocity of tracers. Confocal microscopy (Leica TCS SP5 equipped with an AOBS system) was used to study pumps with photons at different wavelengths (405, 488, 561, and 633 nm) and different powers (5, 25, 50, and 100%). The same confocal microscope was employed for acquiring the fluorescence maps of the concentration of protons with ratiometric measurements. The ratiometric technique minimizes fluorescent artifacts such as the inhomogeneous distribution of the dye.[36] More details on the measurements are reported in the Supporting Information.

Conflict of Interest: The authors declare no competing financial interest.

Supporting Information Available: Eight videos showing the motion of differently charged particles in water and 1% H_2O_2. A pdf file containing the . The Supporting Information is available free of charge on the ACS Publications website at DOI: 10.1021/acsnano.5b04830.

Video captions, details on the ratiometric fluorescent measurements, effect of salt concentration on the pump actuation in water, catalytic performance of p-doped Si/Au pumps, and effect of light wavelength on the actuation mechanism (PDF)

Movie 1 (AVI)
Movie 2 (AVI)
Movie 3 (AVI)
Movie 4 (AVI)
Movie 5 (AVI)
Movie 6 (AVI)
Movie 7 (AVI)
Movie 8 (AVI)

Acknowledgment. We acknowledge M. Roldán and the "Servei de Microscopia" of the UAB for support with fluorescence confocal microscopy measurements. The authors acknowledge support from MINECO and the "Fondo Europeo de Desarrollo Regional" (FEDER) through Grant MAT2012-31338, the European Union (ERC-carbonNEMS project), and the Catalan government (AGAUR, SGR).

REFERENCES AND NOTES

1. Sanchez, S.; Soler, L.; Katuri, J. Chemically Powered Micro- and Nanomotors. *Angew. Chem., Int. Ed.* **2015**, *54*, 1414–1444.
2. Wang, H.; Pumera, M. Fabrication of Micro/Nanoscale Motors. *Chem. Rev.* **2015**, *115*, 8704–8735.
3. Moo, J. G. S.; Pumera, M. Chemical Energy Powered Nano/Micro/Macromotors and the Environment. *Chem. - Eur. J.* **2015**, *21*, 58–723.
4. Colberg, P. H.; Reigh, S. Y.; Robertson, B.; Kapral, R. Chemistry in Motion: Tiny Synthetic Motors. *Acc. Chem. Res.* **2014**, *47*, 3504–3511.
5. Gao, W.; Wang, J. The Environmental Impact of Micro/Nanomachines. A Review. *ACS Nano* **2014**, *8*, 3170–3180.
6. Gao, W.; Wang, J. Synthetic Micro/Nanomotors in Drug Delivery. *Nanoscale* **2014**, *6*, 10486–10494.
7. Sengupta, S.; Patra, D.; Ortiz-Rivera, I.; Agrawal, A.; Shklyaev, S.; Dey, K. K.; Cordova-Figueroa, U.; Mallouk, T. E.; Sen, A. Self-Powered Enzyme Micropumps. *Nat. Chem.* **2014**, *6*, 415–422.
8. Guix, M.; Mayorga-Martinez, C. C.; Merkoci, A. Nano/Micromotors in (Bio)chemical Science Applications. *Chem. Rev.* **2014**, *114*, 6285–6322.
9. Soler, L.; Sanchez, S. Catalytic Nanomotors for Environmental Monitoring and Water Remediation. *Nanoscale* **2014**, *6*, 7175–7182.
10. Wang, W.; Duan, W. T.; Ahmed, S.; Mallouk, T. E.; Sen, A. Small Power: Autonomous Nano- and Micromotors Propelled by Self-Generated Gradients. *Nano Today* **2013**, *8*, 531–554.

11. Sengupta, S.; Ibele, M. E.; Sen, A. Fantastic Voyage: Designing Self-Powered Nanorobots. *Angew. Chem., Int. Ed.* **2012**, *51*, 8434–8445.
12. Mei, Y. F.; Solovev, A. A.; Sanchez, S.; Schmidt, O. G. Rolled-up Nanotech on Polymers: from Basic Perception to Self-Propelled Catalytic Microengines. *Chem. Soc. Rev.* **2011**, *40*, 2109–2119.
13. Ragazzon, G.; Baroncini, M.; Silvi, S.; Venturi, M.; Credi, A. Light-Powered Autonomous and Directional Molecular Motion of a Dissipative Self-Assembling System. *Nat. Nanotechnol.* **2015**, *10*, 70–75.
14. Ma, X.; Tian, H. Bright Functional Rotaxanes. *Chem. Soc. Rev.* **2010**, *39*, 70–80.
15. Feringa, B. L. The Art of Building Small: from Molecular Switches to Molecular Motors. *J. Org. Chem.* **2007**, *72*, 6635–6652.
16. Saha, S.; Stoddart, J. F. Photo-Driven Molecular Devices. *Chem. Soc. Rev.* **2007**, *36*, 77–92.
17. Saha, S.; Leung, K. C. F.; Nguyen, T. D.; Stoddart, J. F.; Zink, J. I. Nanovalves. *Adv. Funct. Mater.* **2007**, *17*, 685–693.
18. Ichimura, K.; Oh, S. K.; Nakagawa, M. Light-Driven Motion of Liquids on a Photoresponsive Surface. *Science* **2000**, *288*, 1624–1626.
19. Barrett, C. J.; Mamiya, J. I.; Yager, K. G.; Ikeda, T. Photo-Mechanical Effects in Azobenzene-Containing Soft Materials. *Soft Matter* **2007**, *3*, 1249–1261.
20. Ube, T.; Ikeda, T. Photomobile Polymer Materials with Crosslinked Liquid-Crystalline Structures: Molecular Design, Fabrication, and Functions. *Angew. Chem., Int. Ed.* **2014**, *53*, 10290–10299.
21. Kondo, M.; Miyasato, R.; Naka, Y.; Mamiya, J.; Kinoshita, M.; Yu, Y. L.; Barrett, C. J.; Ikeda, T. Photomechanical Properties of Azobenzene Liquid-Crystalline Elastomers. *Liq. Cryst.* **2009**, *36*, 1289–1293.
22. Kline, R. T.; Sen, A. Reversible Pattern Formation through Photolysis. *Langmuir* **2006**, *22*, 7124–7127.
23. Chaturvedi, N.; Hong, Y.; Sen, A.; Velegol, D. Magnetic Enhancement of Phototaxing Catalytic Motors. *Langmuir* **2010**, *26*, 6308–6313.
24. Ibele, M. E.; Lammert, P. E.; Crespi, V. H.; Sen, A. Emergent, Collective Oscillations of Self-Mobile Particles and Patterned surfaces under Redox Conditions. *ACS Nano* **2010**, *4*, 4845–4851.
25. Duan, W.; Ibele, M.; Liu, R.; Sen, A. Motion Analysis of Light-Powered Autonomous Silver Chloride Nanomotors. *Eur. Phys. J. E: Soft Matter Biol. Phys.* **2012**, *35*, 77.
26. Ibele, M.; Mallouk, T. E.; Sen, A. Schooling Behavior of Light-Powered Autonomous Micromotors in Water. *Angew. Chem., Int. Ed.* **2009**, *48*, 3308–3312.
27. Duan, W.; Liu, R.; Sen, A. Transition between Collective Behaviors of Micromotors in Response to Different Stimuli. *J. Am. Chem. Soc.* **2013**, *135*, 1280–1273.
28. Hong, Y.; Diaz, M.; Córdova-Figueroa, U. M.; Sen, A. Light-Driven Titanium Dioxide Based Reversible Microfireworks and Micromotor/Micropump Systems. *Adv. Funct. Mater.* **2010**, *20*, 1568–1567.
29. Yadav, V.; Zhang, H.; Pavlick, R.; Sen, A. Triggered "On/Off" Micropumps and Colloidal Photodiode. *J. Am. Chem. Soc.* **2012**, *134*, 15688–15691.
30. Palacci, J.; Sacanna, S.; Kim, S. H.; Yi, G. R.; Pine, D. J.; Chaikin, P. M. Light-Activated Self-Propelled Colloids. *Philos. Trans. R. Soc., A* **2014**, *372*, 20130372.
31. Giudicatti, S.; Marz, S. M.; Soler, L.; Madani, A.; Jorgensen, M. R.; Sanchez, S.; Schmidt, O. G. Photoactive Rolled-up TiO_2 Microtubes: Fabrication, Characterization and Applications. *J. Mater. Chem. C* **2014**, *2*, 5892–5901.
32. Tang, X.; Tang, S.; Sivan, V.; Zhang, W.; Mitchell, A.; Kalantar-Zadeh, K.; Khoshmanesh, K. Photochemically Induced Motion of Liquid Metal Marbles. *Appl. Phys. Lett.* **2013**, *103*, 174104.
33. Palacci, J.; Sacanna, S.; Steinberg, A. P.; Pine, D. J.; Chaikin, P. M. Living Crystal of Light-Activated Colloidal Surfers. *Science* **2013**, *339*, 936–940.
34. Palacci, J.; Sacanna, S.; Vatchinsky, A.; Chaikin, P. M.; Pine, D. J. Photoactivated Colloidal Dockers for Cargo Transportation. *J. Am. Chem. Soc.* **2013**, *135*, 15978–15981.
35. Solovev, A. A.; Smith, E. J.; Bof Bufon, C. C.; Sanchez, S.; Schmidt, O. G. Light-Controlled Propulsion of Catalytic Microengines. *Angew. Chem., Int. Ed.* **2011**, *50*, 10875–10878.
36. Afshar Farniya, A.; Esplandiu, M. J.; Reguera, D.; Bachtold, A. Imaging the Proton Concentration and Mapping the Spatial Distribution of the Electric Field of Catalytic Micropumps. *Phys. Rev. Lett.* **2013**, *111*, 168301.
37. Afshar Farniya, A.; Esplandiu, M. J.; Bachtold, A. Sequential Tasks Performed by Catalytic Pumps for Colloidal Crystallization. *Langmuir* **2014**, *30*, 11841–11845.
38. Kline, T. R.; Paxton, W. F.; Wang, Y.; Velegol, D.; Mallouk, T. E.; Sen, A. Catalytic Micropumps: Microscopic Convective Fluid Flow and Pattern Formation. *J. Am. Chem. Soc.* **2005**, *127*, 17150–17151.
39. Howse, J. R.; Jones, R. A. L.; Ryan, A. J.; Gough, T.; Vafabakhsh, R.; Golestanian, R. Self-Motile Colloidal Particles from Directed Propulsion to Random Walk. *Phys. Rev. Lett.* **2007**, *99*, 048102.
40. Anderson, J. L. Colloid Transport by Interfacial Forces. *Annu. Rev. Fluid Mech.* **1989**, *21*, 61–99.
41. Brown, A.; Poon, W. Ionic Effects in Self-Propelled Pt-Coated Janus Swimmers. *Soft Matter* **2014**, *10*, 4016–4027.
42. Ebbens, S.; Gregory, D. A.; Dunderdale, G.; Howse, J. R.; Ibrahim, Y.; Liverpool, T. B.; Golestanian, R. Electrokinetic Effects in Catalytic Pt-Insulator Janus Swimmers. *Europhys. Lett.* **2014**, *106*, 58003.
43. Linsebigler, A. L.; Lu, G.; Yates, J. T. Photocatalysis on TiO_2 Surfaces: Principles, Mechanisms and Selected Rules. *Chem. Rev.* **1995**, *95*, 735–758.
44. Chandrasekharan, N.; Kamat, P. V. Improving the Photoelectrochemical Performance of Nanostructured TiO_2 Films by Adsorption of Gold Nanoparticles. *J. Phys. Chem. B* **2000**, *104*, 10851–10857.